4920 *Inorg. Chem.* **1991**, *30*, 4920–4927

Contribution from the Biomedical Chemistry Research Center, Department of Chemistry, University of Cincinnati, Cincinnati, Ohio 45221-0172, and Department of Chemistry, Wayne State University, Detroit, Michigan 48202

Synthesis and Characterization of the (Thiolato)rhenium(III) Complexes *trans*-$[Re(SR)_2(R'_2PCH_2CH_2PR'_2)_2]^+$, Where R Is an Alkyl, Benzyl, or Phenyl Group and R′ Is an Ethyl or Phenyl Group. Single-Crystal Structural Analyses of *trans*-$[Re(SC_6H_5)_2(Et_2PCH_2CH_2PEt_2)_2]PF_6$, *trans*-$[Re(SC_6H_4\text{-}p\text{-}CH_3)_2(Et_2PCH_2CH_2PEt_2)_2]PF_6$, and *trans*-$[Re(SC_6H_5)_2(Ph_2PCH_2CH_2PPh_2)_2]CF_3SO_3\cdot{}^1/_2NCCH_3$

Lihsueh (Sherry) Chang,[1] Sen-Ichi Aizawa,[2] Mary Jane Heeg,[3] and Edward Deutsch*,[1]

Received April 18, 1991

The mixed-ligand Re(III) complexes *trans*-$[Re(SR)_2(R'_2PCH_2CH_2PR'_2)_2]^+$ in which R′ = CH_2CH_3 (DEPE) and C_6H_5 (DPPE) while R = CH_2CH_3, $CH_2C_6H_4$-*p*-OCH_3, $CH_2C_6H_5$, C_6H_4-*p*-CH_3, C_6H_5, and C_6H_4-*p*-Cl have been synthesized and characterized. Preparation of these complexes proceeds from the Re(V) complexes *trans*-$[Re(O)Cl_3(PPh_3)_2]$ or *trans*-$[ReO_2Py_4]Cl\cdot 2H_2O$ utilizing excesses of thiol and phosphine as both reductants and ligands. The products are characterized by FAB mass spectroscopy, visible–UV spectroscopy, cyclic voltammetry, and elemental analyses. X-ray crystal structure analyses of prototypical complexes show that they have trans geometry. *trans*-$[Re^{III}(SC_6H_5)_2(DEPE)_2]PF_6$, chemical formula $ReP_5S_2C_{32}H_{58}F_6$, crystallizes in the monoclinic space group $P2_1/a$, with $Z = 2$ and lattice parameters $a = 15.6444$ (9) Å, $b = 13.932$ (7) Å, $c = 9.778$ (3) Å, $\beta = 110.91$ (4)°, and $V = 1990$ (2) Å^3. The final R_1 value is 0.028. *trans*-$[Re^{III}(SC_6H_4\text{-}p\text{-}CH_3)_2(DEPE)_2]PF_6$, chemical formula $ReP_5S_2C_{34}H_{62}F_6$, crystallizes in the monoclinic space group $P2_1/a$, with $Z = 2$ and lattice parameters $a = 11.729$ (3) Å, $b = 15.846$ (2) Å, $c = 12.254$ (2) Å, $\beta = 95.35$ (2)°, $V = 2267.5$ (7) Å^3. The final R_1 value is 0.026. *trans*-$[Re^{III}(SC_6H_5)_2(DPPE)_2]CF_3SO_3\cdot{}^1/_2NCCH_3$, chemical formula $ReP_4S_3F_3O_3N_{0.5}C_{66}H_{59.5}$, crystallizes in the triclinic space group $P\bar{1}$ with $Z = 2$ and lattice parameters $a = 13.318$ (4) Å, $b = 13.341$ (4) Å, $c = 19.763$ (5) Å, $\alpha = 77.82$ (2)°, $\beta = 72.55$ (2)°, $\gamma = 66.02$ (2)°, $V = 3044$ (1) Å^3. The final R_1 value is 0.043. For all three complexes the Re–S bond lengths are similar (2.303, 2.305, and 2.321 Å) with the longest bond length associated with the more electron-donating *p*-tolulenethiolato ligand. Likewise, the Re–P distances are similar (2.45, 2.45, and 2.47 Å), with the longest bond length associated with the more sterically demanding DPPE ligand. These Re(III)–S and Re(III)–P bond lengths are nearly identical to the corresponding Tc(III) bond lengths. The potentials of the reversible Re(III/II) couples depend on the properties of the thiolato and diphosphine ligands and are ca. 0.3 V more negative than those of the analogous Tc(III/II) couples.

Introduction

The chemistry and biodistributions of technetium complexes have attracted much attention due to the wide use of the metastable isotope ^{99m}Tc in diagnostic nuclear medicine. In order to investigate the chemical and physical properties of these ^{99m}Tc complexes, the analogous complexes are prepared on the macroscopic scale with the long-lived technetium isotope ^{99}Tc.

More recently, ^{186}Re complexes have been investigated with regard to their potential use in nuclear medicine.[4] Although analogous technetium and rhenium complexes exhibit similar physical properties, subtle chemical differences between these complexes can result in their exhibiting distinctly different biological behavior.[4,5] Paramount among these chemical differences is the redox behavior of the central metal; complexes of rhenium are more difficult to reduce than are the corresponding technetium complexes. This difference in redox potential can be large enough to shift one complex or the other out of the range of potentials readily accessible to biological systems. This phenomenon has been established by a comparative biodistribution study of the analogous cations $[^{99m}Tc(DMPE)_2Cl_2]^+$ and $[^{186}Re(DMPE)_2Cl_2]^+$.[6,7] The biodistribution data reveal that in vivo reduction occurs for the technetium complex but not for the rhenium analogue. In vivo reduction of the Tc(III) cation converts it to the more lipophilic Tc(II) neutral complex $[^{99m}Tc(DMPE)_2Cl_2]^0$; this causes myocardial washout and unfavorable imaging characteristics.

To elaborate this result, a new class of (thiolato)technetium complexes in which the Tc(III/II) redox potential can be finely tuned has been prepared and characterized.[8-11] Thus, our attention is now focused on sets of analogous complexes, *trans*- or *cis*-$[M^{III}(DIP)_2(SR)_2]^{+/0}$, where M is Tc or Re, DIP represents a tertiary diphosphine chelate such as DMPE, DEPE, or DPPE and R represents an ethyl, benzyl, or phenyl group. Technetium complexes in which DIP is DEPE or DMPE have been well characterized by utilizing macroscopic amounts of ^{99}Tc.[8-11] In this paper we present the synthesis and characterization of a series of thiolato rhenium analogues, $[Re^{III}(DIP)_2(SR)_2]^+$. The study of these (thiolato)rhenium complexes is of interest not only because of their potential applications in nuclear medicine but also because such study will lead to a better understanding of the comparative chemistry of Tc and Re. The interactions between nuclear medicine and inorganic chemistry are truly synergistic.

Acronyms and Abbreviations

The following acronyms and abbreviations are used in this article: DIP = diphosphine; DEPE = 1,2-bis(diethylphosphino)ethane; DMPE = 1,2-bis(dimethylphosphino)ethane; DPPE = 1,2-bis(diphenylphosphino)ethane; DMF = *N*,*N*-dimethylformamide; Et = ethyl; FAB = fast atom bombardment; Ph = phenyl; Py = pyridine; TEAP = tetraethylammonium perchlorate.

Experimental Section

Reagents. All chemicals were of reagent grade unless otherwise noted. The DPPE and DEPE ligands were purchased from Strem Chemical Co. and used without further purification. Ammonium perrhenate, ethanethiol, benzyl mercaptan (α-toluenethiol), toluenethiol (*p*-thiocresol), thiophenol, 4-chlorothiophenol, and 4-methoxyl-α-toluenethiol, were purchased from Aldrich Chemical Co. and used without further purification. Kieselgel (silica gel 60, 230–400 mesh) was purchased from Merck Co. The starting complexes, *trans*-$[Re(O)Cl_3(PPh_3)_2]$ and *trans*-$[ReO_2Py_4]Cl\cdot 2H_2O$, were prepared by literature[12] procedures with

---

(1) University of Cincinnati.

(2) On leave from the Department of Chemistry, Nagoya University, Chickusa, Nagoya 464-01, Japan.

(3) Wayne State University.

(4) Vanderheyden, J.-L.; Heeg, M. J.; Deutsch, E. *Inorg. Chem.* **1985**, *24*, 1666.

(5) Hurst, R. W.; Heineman, W. R.; Deutsch, E. *Inorg. Chem.* **1981**, *20*, 3289.

(6) Kirchhoff, J. R.; Heineman, W. R.; Deutsch, E. *Inorg. Chem.* **1987**, *26*, 3108.

(7) Deutsch, E.; Libson, K.; Vanderheyden, J.-L.; Ketring, A. R.; Maxon, H. R. *Nucl. Med. Biol.* **1986**, *13*, 465.

(8) Konno, T.; Heeg, M. J.; Deutsch, E. *Inorg. Chem.* **1988**, *27*, 4113.

(9) Konno, T.; Kirchhoff, J. R.; Heineman, W. R.; Deutsch, E. *Inorg. Chem.* **1989**, *28*, 1174.

(10) Konno, T.; Heeg, M. J.; Deutsch, E. *Inorg. Chem.* **1989**, *28*, 1694.

(11) Konno, T.; Heeg, M. J.; Seebee, R.; Kirchhoff, J. R.; Heineman, W. R.; Deutsch, E., *Inorg. Chem.*, submitted for publication.

0020-1669/91/1330-4920\$02.50/0

Table I. Experimental Crystallographic Data for $[Re(SC_6H_5)_2(DEPE)_2]PF_6$ (**1**), $[Re(SC_6H_4\text{-}p\text{-}CH_3)_2(DEPE)_2]PF_6$ (**2**), and $[Re(SC_6H_5)_2(DPPE)_2]CF_3SO_3\cdot{}^1/_2(NCCH_3)$ (**3**)

	1	**2**	**3**
formula	$Re_1S_2P_5F_6C_{32}H_{58}$	$Re_1S_2P_5F_6C_{34}H_{62}$	$Re_1S_3P_4F_3O_3N_{0.5}C_{66}H_{59.5}$
fw	962.00	990.06	1371.0
cryst dimens, mm	0.38 × 0.20 × 0.20	0.40 × 0.22 × 0.36	0.20 × 0.15 × 0.35
cryst syst	monoclinic	monoclinic	triclinic
space group	$P2_1/a$	$P2_1/a$	$P\bar{1}$
cell dimens[a]			
a, Å	15.6444 (9)	11.729 (3)	13.318 (4)
b, Å	13.932 (7)	15.846 (2)	13.341 (4)
c, Å	9.778 (3)	12.254 (2)	19.763 (5)
α, deg			77.82 (2)
β, deg	110.91 (4)	95.35 (2)	72.55 (2)
γ, deg			66.02 (2)
V, Å^3	1990 (2)	2267.5 (7)	3044 (1)
Z	2	2	2
d_{calcd}, g cm^{-3}	1.605	1.450	1.495
radiation; λ, Å	Cu Kα; 1.541 78	Mo Kα; 0.710 73	Mo Kα; 0.710 73
scan method	$\theta/2\theta$	$\theta/2\theta$	$\theta/2\theta$
scan rate, deg min^{-1}	4–10	4–10	3–15
2θ range, deg	6–110	6–50	6–50
tot. no. data	2831	4498	11 106
no. of obsd data; range	2246; $I_0 \geq 2.5\sigma(I)$	2971; $I_0 \geq 2.5\sigma(I)$	6889; $I_0 \geq 4\sigma(I)$
hkl ranges	$0 \geq h \geq 16$	$0 \geq h \geq 14$	$0 \geq h \geq 16$
	$0 \geq k \geq 15$	$0 \geq k \geq 19$	$-16 \geq k \geq +16$
	$-11 \geq l \geq +11$	$-15 \geq l \geq +15$	$-24 \geq l \geq +24$
μ, cm^{-1}	91.02	30.23	22.78
transm coeff	0.283–0.175	0.372–0.261	0.909–0.710
F_{000}	972	1004	1386
refinement matrix	full	full	blocked
R_1; R_2	0.028; 0.033	0.026; 0.030	0.043; 0.057
w	$(\sigma_F{}^2 + 0.00005F^2)^{-1}$	$(\sigma_F{}^2 + 0.0001F^2)^{-1}$	$(\sigma_F{}^2 + 0.00005F^2)^{-1}$

the additional modifications specified below. DMF from Burdick and Jackson Laboratories, Inc. and polarographic grade TEAP from G. F. Smith Chemicals were used in the electrochemical measurements. No significant electroactive impurities were detected in either the solvents or the supporting electrolyte.

Measurements. Elemental analyses were performed by Galbraith Laboratories, Knoxville, TN. IR spectra were recorded on a Perkin-Elmer 1600 FT-IR spectrometer in KBr pellets. Visible–UV spectra were recorded in methylene chloride on a Cary 210 spectrophotometer (Varian) at room temperature. FAB mass spectra were measured in the positive ion mode using a VG 30-250 spectrometer (VG Instruments Inc.) and *m*-nitrobenzyl alcohol (NBA) matrix at the probe temperature. Xenon was used as the primary beam gas, and the ion gun was operated at 7 kV and 1 mA. Data were generally collected over the mass range 100–1500 Da at 3 s/scan. Electrochemical measurements were made with a Bioanalytical Systems, Inc. (BAS), 100A apparatus using a glassy-carbon-disk working electrode; an aqueous Ag/AgCl (3 M NaCl) electrode (BAS) and platinum wire were used as the reference and auxiliary electrodes respectively. All potentials are reported versus this reference electrode. The electrochemical experiment was conducted in DMF with 0.5 M TEAP as supporting electrolyte, at a complex concentration of ca. 1 mM.

Crystallography. X-ray diffraction experiments were performed on a Nicolet R3 or P2$_1$ automated diffractometer equipped with a graphite monochromator at ambient temperature using the $\theta/2\theta$ scan method. The structures were solved by Patterson methods and defined with the programs of SHELX-76.[13] Neutral-atom scattering factors and corrections for anomalous dispersions were from ref 14. Absorption corrections were by empirical methods.[15] Experimental details are given in Table I.

***trans*-$[Re(SC_6H_5)_2(DEPE)_2]PF_6$.** The final refinement model included anisotropic non-hydrogen atoms and invariant hydrogen atoms.

***trans*-$[Re(SC_6H_4\text{-}p\text{-}CH_3)_2(DEPE)_2]PF_6$.** All non-hydrogen atoms in the cation and anion were refined anisotropically; the partial occupancy oxygen atoms of the disordered solvent were described isotropically only. Hydrogen atoms were placed in observed positions and held invariant. One reflection (200) was omitted on the basis of secondary extinction.

***trans*-$[Re^{III}(SC_6H_5)_2(DPPE)_2]CF_3SO_3\cdot{}^1/_2(NCCH_3)$.** All non-hydrogen atoms of the cation were refined anisotropically. Phenyl rings were defined as rigid bodies. Isotropic refinement was carried out on the anion and solvent. Hydrogen atoms were placed in calculated positions and held invariant, defining $U(H) = 1.5\,U(C)$ of the carbon to which it is bound.

Synthesis. *trans*-Monooxotrichlorobis(triphenylphosphine)rhenium(V),[12] *trans*-$[ReOCl_3(PPh_3)_2]$. A suspension of triphenylphosphine (16 g, 61 mmol) in glacial acetic acid (150 mL) was heated to 90 °C to form a clear solution. To this solution at 90 °C, NH_4ReO_4 (1.00 g, 3.72 mmol) in concentrated HCl (32 mL) was added dropwise over a 10-min period. After complete addition, this mixture was heated at 90 °C overnight. The resulting solid was collected by filtration and washed with acetic acid (3 × 30 mL) and ethyl ether (3 × 50 mL) to provide a dry green solid (3.10 g, 3.72 mmol) in quantitative yield. The trans geometry of this green solid was confirmed by IR (KBr, pellet): Re=O, ν = 980 cm^{-1} (lit.:[12] Re=O, ν = 981 cm^{-1}).

***trans*-Dioxotetrakis(pyridine)rhenium(V) Chloride Dihydrate, *trans*-$[ReO_2Py_4]Cl\cdot 2H_2O$,** was prepared by the method described in ref 12. FAB-MS analysis showed the presence of the ion $[ReO_2Py_4]^+$. This product was used without any further purification as a starting material in the syntheses of $[Re(SR)_2(DIP)_2]CF_3SO_3$ complexes.

***trans*-Dioxobis(1,2-bis(diphenylphosphino)ethane)rhenium(V) Chloride,[16] *trans*-$[ReO_2(DPPE)_2]Cl$.** To a stirred solution of $[ReO_2Py_4]Cl\cdot 2H_2O$ (400 mg, 0.66 mmol) in ethanol (15 mL) was added a solution of DPPE (650 mg, 1.63 mmol) in CH_2Cl_2 (5 mL) dropwise. This mixture was then heated to reflux for 3 h. The resulting solution was concentrated by evaporation to a volume of about 5 mL. Slow addition of diethyl ether yielded yellow crystals. These crystals were collected by filtration and washed with diethyl ether (50 mL). Positive ion FAB-MS (*m/z*, ion): $[ReO_2(DPPE)_2]^+$ at 1015/1013 Da ($^{187}Re/^{185}Re$), M$^+$ (parent peak). IR (KBr, pellet): Re=O, ν = 788 cm^{-1} (lit.:[16] Re=O, ν = 788 cm^{-1}).

Bis(thiolato)bis(1,2-bis(diphenylphosphino)ethane)rhenium(III) Trifluoromethanesulfonate, $[Re(SR)_2(DPPE)_2]CF_3SO_3$ (R = Ethyl, Benzyl, *p*-Methoxybenzyl, Phenyl, *p*-Methylphenyl, *p*-Chlorophenyl). Method A. Preparation from *trans*-$[ReO_2Py_4]Cl\cdot 2H_2O$. To a stirred solution of $[ReO_2Py_4]Cl\cdot 2H_2O$ (200 mg, 0.35 mmol) in ethanol (5 mL) at 60 °C

---

[12] Johnson, N. P.; Lock, C. J. L.; Wilkinson, G. *J. Chem. Soc.* **1964**, 1054.

[13] Sheldrick, G. M. SHELX-76. University Chemical Laboratory, Cambridge, England, 1976.

[14] *International Tables for X-ray Crystallography*; Kynoch: Birmingham, England, 1974; Vol. 4 (present distributor D. Reidel, Dordrecht, The Netherlands).

[15] Sheldrick, G. M. SHELXTL. University of Göttingen, Göttingen, Federal Republic of Germany, 1978.

[16] Freni, M.; Giusto, D.; Romiti, P.; Minghetti, G. *Gazz. Chim. Ital.* **1969**, *99*, 286.

[17] Jones, W. D.; Maguire, J. A. *Organometallics* **1987**, *6*, 1728.

[18] Libson, K.; Barnett, B. L.; Deutsch, E. *Inorg. Chem.* **1983**, *22*, 1695.

[19] Libson, K.; Doyle, M. N.; Thomas, R. W.; Nelesnik, T.; Woods, M.; Sullivan, J. C.; Elder, R. C.; Deutsch, E. *Inorg. Chem.* **1988**, *27*, 3614.

Table II. Colors, Isolated Yields, and UV-Visible Data for $[Re(SR)_2(DIP)_2]^+$ Products

starting material[a]	product	color	% isolated yield	$\lambda_{max}/10^3$ cm^{-1}	$\epsilon/10^3$ M^{-1} cm^{-1}
A	$[Re(SCH_2CH_3)_2(DPPE)_2]CF_3SO_3$	red	b	19.80	25.09
B	$[Re(SCH_2CH_3)_2(DPPE)_2]CF_3SO_3$	red	14[c]	30.30 sh[d]	8.96
				33.11 sh[d]	21.50
				34.84	26.43
A	$[Re(SCH_2C_6H_4\text{-}p\text{-}OCH_3)_2(DPPE)_2]CF_3SO_3$	red	75	19.53	34.82
B	$[Re(SCH_2C_6H_4\text{-}p\text{-}OCH_3)_2(DPPE)_2]CF_3SO_3$	red	61	30.49 sh[d]	10.79
				35.09	37.99
A	$[Re(SCH_2C_6H_5)_2(DPPE)_2]CF_3SO_3$	red	68	19.57	28.63
B	$[Re(SCH_2C_6H_5)_2(DPPE)_2]CF_3SO_3$	red	68	30.49 sh[d]	9.62
				34.84	29.23
A	$[Re(SC_6H_4\text{-}p\text{-}CH_3)_2(DPPE)_2]CF_3SO_3$	blue	89	16.10	38.16
B	$[Re(SC_6H_4\text{-}p\text{-}CH_3)_2(DPPE)_2]CF_3SO_3$	blue	<14	20.96	2.10
				26.18	2.88
				35.71 sh[d]	35.40
A	$[Re(SC_6H_5)_2(DPPE)_2]CF_3SO_3$	blue	80	16.47	30.12
B	$[Re(SC_6H_5)Cl(DPPE)_2]^+$	green	b	20.92	1.38
				26.32	2.26
				33.78 sh[d]	12.97
				37.74 sh[d]	23.46
A	$[Re(SC_6H_4\text{-}p\text{-}Cl)_2(DPPE)_2]CF_3SO_3$	blue	61[c]	16.26	36.99
B	$[Re(SC_6H_4\text{-}p\text{-}Cl)Cl(DPPE)_2]^+$	green	b	20.92	1.60
				25.51	2.91
				35.46	27.11
A	$[Re(SCH_2CH_3)_2(DEPE)_2]PF_6$	red	small	19.65	20.96
B	$[Re(SCH_2CH_3)_2(DEPE)_2]CF_3SO_3$	red	small	31.45	2.21
A	$[Re(SCH_2C_6H_4\text{-}p\text{-}OCH_3)_2(DEPE)_2]PF_6$	red	26	19.31	22.21
				34.36	13.59
				42.19	52.29
A	$[Re(SCH_2C_6H_5)_2(DEPE)_2]CF_3SO_3$	red	23	19.34	23.41
B	$[Re(SCH_2C_6H_5)_2(DEPE)_2]PF_6$	red	42	33.22	11.42
				38.91 sh[d]	10.81
A	$[Re(SC_6H_4\text{-}p\text{-}CH_3)_2(DEPE)_2]PF_6$	purple	54	17.21	20.79
				19.23 sh[d]	11.55
				27.47 sh[d]	2.93
				31.06 sh[d]	3.71
				39.22	41.18
A	$[Re(SC_6H_5)_2(DEPE)_2]PF_6$	purple	60	17.57	24.99
				19.34 sh[d]	15.36
				27.62 sh[d]	3.70
				31.06 sh[d]	4.53
				39.37	50.32
A	$[Re(SC_6H_4\text{-}p\text{-}Cl)_2(DEPE)_2]PF_6$	purple	34	17.39	24.99
				19.26	13.56
				27.17 sh[d]	4.26
				31.06 sh[d]	5.60
				38.37	46.66

[a] Key: (A) $[ReO_2Py_4]Cl\cdot 2H_2O$; (B) $[Re(O)Cl_3(PPh_3)_2]$. [b] The product was not isolated and no UV-visible data were obtained. [c] After recrystallization. [d] sh denotes a shoulder.

Table III. FAB Mass Spectral Data (*m/e*) for $[Re(SR)_2(DIP)_2]^+$ Complexes

	complex ion, M^+	fragment ion					
		M − R	M − 2R	M − SR	M − DIP	M − DIP, R	M − DIP, 2R
$[Re(SCH_2CH_3)_2(DPPE)_2]^+$	1105/1103				705	677	649[a]
$[Re(SCH_2C_6H_4\text{-}p\text{-}OCH_3)_2(DPPE)_2]^+$	1289/1287		1047				649[a]
$[Re(SCH_2C_6H_5)_2(DPPE)_2]^+$	1229/1227		1047				649[a]
$[Re(SC_6H_4\text{-}p\text{-}CH_3)_2(DPPE)_2]^+$	1229/1227				831[a]		649
$[Re(SC_6H_5)_2(DPPE)_2]^+$	1201/1199				803[a]		649
$[Re(SC_6H_4\text{-}p\text{-}Cl)_2(DPPE)_2]^+$	1269/1267[b]				871[a]		649
$[Re(SCH_2CH_3)_2(DEPE)_2]^+$	721/719		663				457[a]
$[Re(SCH_2C_6H_4\text{-}p\text{-}OCH_3)_2(DEPE)_2]^+$	905/903	784	663[a]				
$[Re(SCH_2C_6H_5)_2(DEPE)_2]^+$	845/843	753	663[a]		639		
$[Re(SC_6H_4\text{-}p\text{-}CH_3)_2(DEPE)_2]^+$	845[a]/843		663	723	639		
$[Re(SC_6H_5)_2(DEPE)_2]^+$	817/815			708	611[a]		
$[Re(SC_6H_4\text{-}p\text{-}Cl)_2(DEPE)_2]^+$	885[a]/883[b]			742	679	711	

[a] Base peak. [b] The isotope pattern due to $^{187/185}Re$ and $^{37/35}Cl$ is observed as expected.

was added an excess of RSH (2.10 mmol). This solution was stirred at 60 °C for 5 min, and then a solution of DPPE (400 mg, 1.05 mmol) in CH_2Cl_2 (3 mL) was added under argon. This reaction mixture was heated at 60 °C for 2–3 h; the solution became deep red in color when R = ethyl, benzyl, or *p*-methoxybenzyl, and deep blue in color when R = phenyl, *p*-methylphenyl or *p*-chlorophenyl. The resulting mixture was filtered to remove any precipitate, and 2 mL of a saturated solution of $LiCF_3SO_3$ in ethanol was added dropwise. This solution was concentrated to 5 mL by evaporation at 60 °C and water (0.2–0.3 mL) was added dropwise to form crystals of $[Re(SR)_2(DPPE)_2]CF_3SO_3$. These crystals were collected by filtration and washed with ethanol (1 mL) and water (2 × 3 mL) to remove excess ligands and $LiCF_3SO_3$. The yields of the isolated products are listed in Table II; FAB-MS data are given in Table III.

Table IV. Electrochemical Data for *trans*-$[Re(SR)_2(DIP)_2]^+$ Complexes in 0.5 M TEAP in DMF[a,b]

	Re(IV/III)		Re(III/II)	Re(II/I)[c]	
	E_{pa}	E_{pc}	$E^{\circ\prime}$	E_{pc}	E_{pa}
$[Re(SCH_2CH_3)_2(DPPE)_2]^+$	1098	1008	−744	−1780	
$[Re(SCH_2C_6H_4\text{-}p\text{-}OCH_3)_2(DPPE)_2]^+$	1056	...	−681	−1746	
$[Re(SCH_2C_6H_5)_2(DPPE)_2]^+$	959	...	−653	−1708	
$[Re(SC_6H_5\text{-}p\text{-}CH_3)_2(DPPE)_2]^+$	1054	954	−620	−1608	
$[Re(SC_6H_5)_2(DPPE)_2]^+$	1170[d]	1030[d]	−553	−1524[d]	−1395[d]
$[Re(SC_6H_4\text{-}p\text{-}Cl)_2(DPPE)_2]^+$			−443	−1447	−1390
$[Re(SCH_2CH_3)_2(DEPE)_2]^+$	849	...	−894		
$[Re(SCH_2C_6H_4\text{-}p\text{-}OCH_3)_2(DEPE)_2]^+$	789	...	−850		
$[Re(SCH_2C_6H_5)_2(DEPE)_2]^+$	950	...	−822		
$[Re(SC_6H_5\text{-}p\text{-}CH_3)_2(DEPE)_2]^+$		...	−605	−1730	−1652
$[Re(SC_6H_5)_2(DEPE)_2]^+$			−573	−1610	
$[Re(SC_6H_4\text{-}p\text{-}Cl)_2(DEPE)_2]^+$			−532	−1608[e]	−1535

[a] 25 °C; glassy-carbon working electrode; scan rate 100 mV/s; all values in mV. [b] $E^{\circ\prime} = (E_{pc} + E_{pa})/2$ vs Ag/AgCl (3 M NaCl) from cyclic voltammetry. [c] Irreversible oxidation at 25 °C. [d] Becomes chemically reversible at −78 °C. [e] Reversible oxidation at 25 °C.

When R = phenyl, *p*-methylphenyl, and *p*-chlorophenyl, a small amount of $[Re(SR)Cl(DPPE)_2]CF_3SO_3$ complexes are formed. These byproducts were characterized by FAB-MS but proved very difficult to isolate and purify due to their high solubility in ethanol and contamination by the major product $[Re(SR)_2(DPPE)_2]CF_3SO_3$.

Method B. Preparation from *trans*-$[ReOCl_3(PPh_3)_2]$. To a suspension of $[ReOCl_3(PPh_3)_2]$ (100 mg, 0.12 mmol) in ethanol (5 mL) at 60 °C was added an excess of RSH (0.72 mmol) and DPPE (140 mg, 0.36 mmol) in CH_2Cl_2 (3 mL) under argon. This mixture was stirred at 60 °C for 2–3 h; the solution became either deep red or bluish green in color as in method A above. This resulting mixture was filtered to remove any precipitate, and then 2 mL of a saturated $LiCF_3SO_3$ solution in EtOH were added. The products were crystallized as above. In the case of R = phenyl, *p*-methylphenyl, and *p*-chlorophenyl, the major product is $[Re(SR)Cl(DPPE)_2]CF_3SO_3$ and the minor product is $[Re(SR)_2(DPPE)_2]CF_3SO_3$. Descriptions of the isolated products and their UV–visible data are given in Table II. Characterization data (FAB-MS, cyclic voltammetry and elemental analyses) are listed in Tables III–V (respectively).

Bis(thiolato)bis(1,2-bis(diethylphosphino)ethane)rhenium(III) Salts, $[Re(SR)_2(DEPE)_2]X$ ($X = CF_3SO_3$, PF_6) (R = Ethyl, Benzyl, *p*-Methoxybenzyl, Phenyl, *p*-Methylphenyl, *p*-Chlorophenyl). The procedures used to prepare these complexes are the same as described above for $[Re(SR)_2(DPPE)_2]CF_3SO_3$ except that neat DEPE under argon was used instead of DPPE in ethanol and that NH_4PF_6 in water was also used to generate crystalline products.

Purification. All of the $[Re(SR)_2(DPPE)_2]X$ salts ($X = CF_3SO_3$, PF_6) were purified by crystallization from CH_2Cl_2/ethanol except that wherein R = Et (which was purified by chromatography; see below). If necessary, a few drops of water were added to initiate crystallization. Complete crystallization occurs over 1 or 2 days, and the crystals are stable within the supernatant for at least 2 weeks. For the DEPE complexes, two crystallizations are required to obtain a pure product.

$[Re(SCH_2CH_3)_2(DPPE)_2]PF_6$ usually contained a white solid impurity which could not be removed by recrystallization. Thus, this red complex was purified using a column (2.5 × 15 cm) packed with silica gel in CH_2Cl_2. After loading, CH_2Cl_2 (~50 mL) was used to remove the colorless impurity; 1/1 (v/v) $CH_3C(O)CH_3/CH_2Cl_2$ was then used to elute the red $[Re(SCH_2CH_3)_2(DPPE)_2]PF_6$. Solvent evaporation yielded the pure complex. $[Re(SC_6H_4\text{-}p\text{-}CH_3)_2(DEPE)_2[PF_6$ was similarly purified on a silica gel column using 1/1 (v/v) $CH_3C(O)CH_3/CH_2Cl_2$ eluent.

Attempts to separate $[Re(SC_6H_4\text{-}p\text{-}Cl)Cl(DPPE)_2]CF_3SO_3$ from a mixture of $[Re(SC_6H_4\text{-}p\text{-}Cl)_{2-n}Cl_n(DPPE)_2]CF_3SO_3$ ($n = 0, 1$) by silica gel chromatography were unsuccessful due to decomposition and the resulting contamination by $[Re(SC_6H_4\text{-}p\text{-}Cl)_2(DPPE)_2]CF_3SO_3$.

Table V. Elemental Analyses for Rhenium Complexes

		elem anal.			
compound		% C	% H	% P	% S
$[Re(SCH_2CH_3)_2(DPPE)_2]CF_3SO_3$	calcd	54.58	4.66	9.88	
	found	54.11	4.73	9.77	
$[Re(SCH_2C_6CH_4\text{-}p\text{-}OCH_3)_2\text{-}(DPPE)_2]CF_3SO_3$	calcd	57.61	4.62	8.61	6.69
	found	56.99	4.83	8.48	6.81
$[Re(SCH_2C_6H_5)_2(DPPE)_2]\text{-}CF_3SO_3$	calcd	58.38	4.53	8.99	6.98
	found	58.37	4.55	9.05	7.00
$[Re(SC_6H_4\text{-}p\text{-}CH_3)_2(DPPE)_2]\text{-}CF_3SO_3$	calcd	58.38	5.53	8.99	6.98
	found	57.93	4.68	8.82	7.03
$[Re(SC_6H_5)_2(DPPE)_2]CF_3SO_3\cdot CH_2Cl_2$	calcd	55.23	4.21	8.63	6.70
	found	54.32	4.18	8.56	6.81
$[Re(SC_6H_4\text{-}p\text{-}Cl)_2(DPPE)_2]\text{-}CF_3SO_3$	calcd	55.01	3.98	8.73	6.78
	found	54.47	3.94	8.41	7.23
$[Re(SCH_2C_6H_4\text{-}p\text{-}OCH_3)_2\text{-}(DEPE)_2]PF_6$	calcd	41.18	6.33	14.75	
	found	41.04	6.32	14.60	
$[Re(SCH_2C_6H_5)_2(DEPE)_2]PF_6$	calcd	41.25	6.31	15.64	
	found	40.56	6.18	15.66	
$[Re(SC_6H_4\text{-}p\text{-}CH_3)_2(DEPE)_2]PF_6$	calcd	41.25	6.31	15.64	
	found	39.69	6.14	14.79	
$[Re(SC_6H_5)_2(DEPE)_2]BPh_4$	calcd	59.20	6.92	10.90	
	found	58.36	6.94	10.36	
$[Re(SC_6H_4\text{-}p\text{-}Cl)_2(DEPE)_2]PF_6$	calcd	37.28	5.48	15.02	
	found	37.38	5.69	14.69	

Results

Synthesis. The *trans*-$[Re^{III}(SR)_2(DIP)_2]X$ complexes (R = C_2H_5, $CH_2C_6H_5$, $CH_2C_6H_4\text{-}p\text{-}OCH_3$, $C_6H_4\text{-}p\text{-}CH_3$, C_6H_5, and $C_6H_4\text{-}p\text{-}Cl$; DIP = DPPE, DEPE; X = CF_3SO_3, PF_6), have been prepared by a general method which was optimized with respect to starting material, pH, reaction temperature, and reaction time by using the complexes with R = C_2H_5 as prototypes. Reduction of Re^V to Re^{III} is dependent on pH. The preparation of $[Re^{III}(SEt)_2(DPPE)_2]^+$ involves sequential addition of first HSC_2H_5 and then DPPE to a solution containing $[ReO_2Py_4]Cl\cdot 2H_2O$ (or $ReOCl_3(PPh_3)_2$) in ethanol at 60 °C. The reverse order of addition provides $[Re^VO_2(DPPE)_2]Cl$ (II) in 2 h. Reaction of excess ethanethiol with the Re(V) complex *trans*-$[Re(O)_2(DPPE)_2]^+$ under anaerobic conditions leads to no detectable thiolato complexes in 2 h at 60 °C. Extending the reaction time to 20 h provides a dark brown solution which does not contain any of the expected product. Purification by recrystallization succeeds for all DPPE complexes except that wherein R = ethyl. A white impurity which coprecipitates during the recrystallization of $[Re(SEt)_2(DPPE)_2]CF_3SO_3$ can be removed by silica gel chromatography. When *trans*-$[Re(O)Cl_3(PPh_3)_2]$ is used as starting material, the green byproduct, $[Re^{III}(SR)Cl(DPPE)_2]^+$ is usually obtained for R = $C_6H_4\text{-}p\text{-}CH_3$, C_6H_5, or $C_6H_4\text{-}p\text{-}Cl$. Thus for these complexes, the starting material *trans*-$[ReO_2Py_4]Cl\cdot 2H_2O$ is used to minimize the formation of $[Re^{III}(SR)Cl(DPPE)_2]^+$. On the other hand, *trans*-$[Re(O)Cl_3(PPh_3)_2]$ is a convenient starting material for the preparation of $[Re(SR)_2(DIP)_2]CF_3SO_3$ (R = alkyl, benzyl; DIP = DPPE, DEPE) in good yield.

Characterization. The thiolato–Re(III) complexes are characterized by (i) elemental analyses of representative compounds, the results of which are in acceptable agreement with the proposed formulations (Table V), (ii) FAB mass spectrometry, (iii) visible–UV spectrophotometry, (iv) cyclic voltammetry, and (v) selected single-crystal X-ray structure analyses.

Compositional assignments for the $[Re^{III}(SR)_2(DIP)_2]^+$ (DIP = DPPE, DEPE) cations are most readily made by a positive ion FAB mass spectrometry (Table III). The positive ion FAB mass spectra show the expected m/z values for the parent ions at M + 2^+ and M^+; the M + $2^+/M^+$ peak height ratio is 2/1 as expected for $^{187/185}Re$. A positive ion FAB mass spectrum of the green complex $[Re^{III}(SR)Cl(DPPE)_2]^+$ shows the pattern of m/z values calculated for this formulation with the natural abundance of

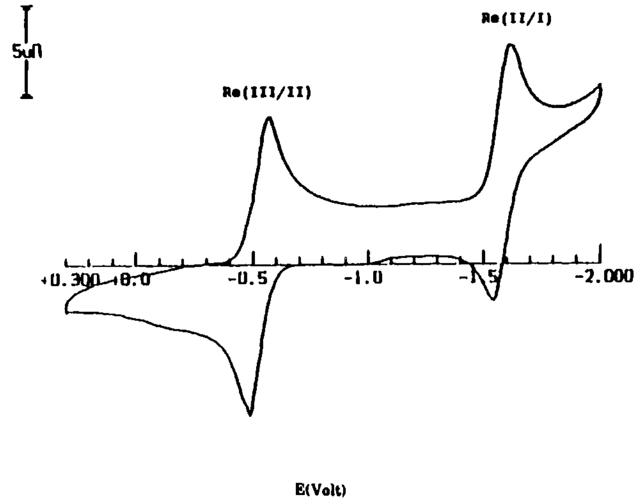

Figure 1. Cyclic voltammogram of 1 mM of $[Re^{I/II/III}(SC_6H_5)_2(DEPE)_2]^{-/0/+}$ in 0.5 M TEAP in DMF at a glassy-carbon electrode. The scan rate is 100 mV/s.

$^{187/185}Re$ and $^{37/35}Cl$ isotopes. The positive ion FAB mass spectrum of $[Re^{III}(SR)Cl(DPPE)_2]^+$ shows that it is contaminated with a small amount of $[Re^{III}(SR)_2(DPPE)_2]^+$.

Several fragment ions corresponding to losses of R or 2R, and DPPE, from *trans*-$[Re^{III}(SR)_2(DPPE)_2]^+$ (R = C_2H_5, $CH_2C_6H_5$, $CH_2C_6H_4$-*p*-OCH_3) are observed; the base peak corresponds to the loss of DPPE and 2R. For the complexes of arene thiols, the base peak corresponds to the loss of a DPPE ligand, while for the complexes of alkyl and benzyl thiols, the base peak corresponds to the loss of 2R. It is noteworthy that fragment ions arising from the loss of a DPPE (or DEPE) ligand are not observed in the phenylmethanethiolato–Re(III) system.

All $[Re^{III}(SR)_2(DIP)_2]^+$ complexes exhibit similar, characteristic, well-defined, intense absorption bands in the visible region.

Electrochemistry. The *trans*-$[Re^{III}(SR)_2(DIP)_2]^+$ complexes have been further characterized by cyclic voltammetry, and the results are summarized in Table IV. The redox behavior of the (thiolato)rhenium complexes is characterized by the three couples Re(II/I), Re(III/II), and Re(IV/III). A typical cyclic voltammogram showing the Re(II/I) and Re(III/II) couples of $[Re^{I/II/III}(SC_6H_5)_2(DEPE)_2]^{-/0/+}$ is given in Figure 1.

All complexes studied in this work exhibit reversible or quasireversible Re(III/II) redox couples: conditions for reversibility are stated in ref 6. The DPPE complexes exhibit Re(III/II) redox potentials more positive than those of analogous DEPE complexes. For complexes containing the same DIP ligand, the Re(III/II) potential depends on the nature of the thiolato ligands (potential values increase in the order ^-SEt < $^-SCH_2C_6H_4$-*p*-OCH_3 < $^-SCH_2C_6H_5$ < $^-SC_6H_4$-*p*-CH_3 < $^-SC_6H_5$ < $^-SC_6H_4$-*p*-Cl). The irreversible Re(II/I) and Re(IV/III) couples tend to become reversible at low temperature; for example, the $[Re(SC_6H_5)_2(DPPE)_2]^{-/0}$ and $[Re(SC_6H_5)_2(DPPE)_2]^{+/+2}$ couples are reversible at −70 °C.

Crystallography. $[Re(SC_6H_5)_2(DEPE)_2]PF_6$. Fractional atomic coordinates are given in Table VI. Selected bond lengths and angles are listed in Table VII for the cation. Figure 2 illustrates the geometry and atom labeling of $[Re(SC_6H_5)_2(DEPE)_2]^+$. The structure consists of an independent half-cation and half-anion; both the Re atom and the P atom of the anion occupy crystallographic inversion centers. The arrangement of the ligating atoms around Re can be adequately described as trans octahedral.

$[Re(SC_6H_4$-*p*-$CH_3)_2(DEPE)_2]PF_6$. Fractional atomic coordinates are given in Table VIII. Selected bond lengths and angles for the cation are listed in Table VII. The trans-octahedral geometry of the cation is shown in Figure 3. The Re atom occupies a crystallographic inversion center. There is an independent half-molecule of PF_6 in the asymmetric unit. This PF_6 anion occurs on a general position in the cell with only half the sites occupied. The remaining half-sites not occupied by PF_6 most likely are occupied by solvent: CH_2Cl_2, ethanol, and/or water. Because of the overlap with PF_6, this solvent region is impossible to sort out and characterize. In the model used herein, five $^1/_4$-occupancy oxygen atoms (O1–O5) have been placed to

Table VI. Fractional Atomic Coordinates for $[Re(SC_6H_5)_2(DEPE)_2](PF_6)$

atom	*x*	*y*	*z*
Re1	0.00000	0.00000	1.00000
S1	0.08190 (8)	0.0445 (1)	0.8555 (1)
P1	0.10923 (8)	−0.11762 (9)	1.1492 (1)
P2	0.08207 (9)	0.1040 (1)	1.2097 (1)
C1	0.1977 (3)	0.0154 (3)	0.8809 (5)
C2	0.2128 (4)	−0.0099 (4)	0.7548 (6)
C3	0.3006 (4)	−0.0285 (5)	0.7592 (7)
C4	0.3722 (4)	−0.0227 (4)	0.8864 (8)
C5	0.3582 (4)	0.0026 (4)	1.0124 (7)
C6	0.2713 (4)	0.0212 (4)	1.0092 (6)
C7	0.0710 (4)	−0.2121 (4)	1.2454 (6)
C8	0.0095 (4)	−0.2854 (5)	1.1502 (7)
C9	0.1801 (3)	−0.1888 (4)	1.0725 (6)
C10	0.2640 (4)	−0.2342 (5)	1.1820 (7)
C11	0.1921 (4)	−0.0554 (4)	1.3082 (5)
C12	0.1438 (4)	0.0241 (4)	1.3602 (5)
C13	0.0123 (4)	0.1779 (5)	1.2847 (7)
C14	0.0492 (8)	0.2020 (9)	1.4433 (9)
C15	0.1671 (4)	0.1898 (4)	1.1918 (7)
C16	0.2492 (5)	0.2109 (6)	1.327 (1)
P3	0.00000	0.50000	0.50000
F1	0.0745 (4)	0.4363 (5)	0.6036 (7)
F2	0.0663 (5)	0.5710 (7)	0.477 (1)
F3	0.0035 (7)	0.4434 (5)	0.3690 (7)

Table VII. Selected Bond Lengths (Å) and Angles (deg) for $[Re^{III}(SC_6H_5)_2(DEPE)_2]^+$ in **1**, and $[Re(SC_6H_4$-*p*-$CH_3)_2(DEPE)_2]^+$ in **2**

1		2	
Re1–S1	2.305 (1)	Re1–S1	2.321 (1)
Re1–P1	2.440 (1)	Re1–P1	2.431 (1)
Re1–P2	2.465 (1)	Re1–P2	2.473 (1)
S1–C1	1.786 (5)	S1–C1	1.800 (5)
Re1–S1–C1	127.8 (1)	Re1–S1–C1	125.7 (2)
Re1–P1–C7	120.1 (2)	Re1–P1–C8	117.3 (2)
Re1–P1–C9	121.0 (1)	Re1–P1–C10	118.9 (2)
Re1–P1–C11	108.6 (2)	Re1–P1–C12	108.1 (2)
Re1–P2–C12	106.3 (2)	Re1–P2–C13	108.9 (2)
Re1–P2–C13	117.1 (2)	Re1–P2–C14	118.8 (2)
Re1–P2–C15	118.8 (1)	Re1–P2–C16	119.2 (2)
S1–Re1–P1	97.08 (4)	S1–Re1–P1	86.87 (4)
S1–Re1–P2	96.51 (4)	S1–Re1–P2	88.30 (4)
P1–Re1–P2	81.47 (4)	P1–Re1–P2	80.78 (4)

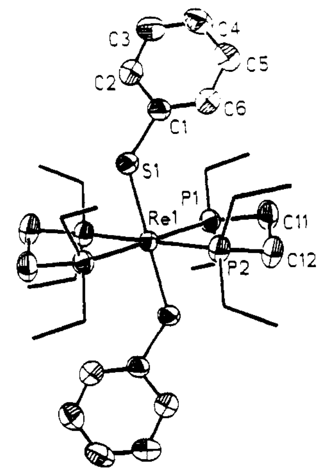

Figure 2. ORTEP diagram of $[Re(SC_6H_5)_2(DEPE)_2]^+$ with ellipsoids at 50% probability. The Re atom occupies an inversion center. The ethyl substitutents on the P atoms have been omitted for clarity but are labeled C7–C10 and C13–C16 in the tables.

Table VIII. Fractional Atomic Coordinates for $[Re(SC_6H_4\text{-}p\text{-}CH_3)_2(DEPE)_2](PF_6)$

atom	*x*	*y*	*z*
Re1	0.00000	0.00000	0.00000
S1	0.1224 (1)	0.11384 (8)	0.0357 (1)
P1	0.0103 (1)	0.03008 (8)	−0.1933 (1)
P2	0.1691 (1)	−0.08658 (9)	−0.0322 (1)
C1	0.1657 (4)	0.1569 (3)	0.1691 (4)
C2	0.2728 (4)	0.1385 (3)	0.2172 (4)
C3	0.3157 (5)	0.1786 (4)	0.3143 (5)
C4	0.2522 (5)	0.2374 (4)	0.3647 (4)
C5	0.3009 (6)	0.2813 (4)	0.4676 (5)
C6	0.1440 (5)	0.2564 (4)	0.3149 (4)
C7	0.1014 (4)	0.2176 (3)	0.2187 (4)
C8	0.0920 (5)	0.1240 (3)	−0.2282 (4)
C9	0.0990 (6)	0.1441 (5)	−0.3468 (5)
C10	−0.1246 (4)	0.0391 (4)	−0.2842 (4)
C11	−0.1297 (5)	−0.0024 (4)	−0.3963 (4)
C12	0.0902 (4)	−0.0557 (3)	−0.2522 (4)
C13	0.1973 (5)	−0.0764 (4)	−0.1774 (4)
C14	0.1620 (5)	−0.2011 (3)	−0.0130 (5)
C15	0.1718 (5)	−0.2293 (4)	0.1060 (6)
C16	0.3089 (4)	−0.0594 (4)	0.0391 (5)
C17	0.4098 (5)	−0.1099 (4)	0.0020 (5)
P3	0.5239 (4)	−0.0653 (4)	0.3442 (4)
F1	0.528 (1)	0.0103 (8)	0.261 (1)
F2	0.436 (1)	−0.0197 (9)	0.369 (1)
F3	0.521 (1)	−0.1091 (9)	0.4462 (9)
F4	0.618 (1)	−0.013 (1)	0.382 (1)
F5	0.615 (2)	−0.116 (2)	0.300 (2)
F6	0.447 (2)	−0.1467 (9)	0.306 (2)
O1	0.572 (2)	−0.003 (2)	0.305 (2)
O2	0.427 (2)	−0.134 (2)	0.358 (2)
O3	0.547 (2)	−0.038 (2)	0.237 (2)
O4	0.520 (4)	−0.152 (3)	0.328 (3)
O5	0.415 (2)	−0.105 (2)	0.298 (3)

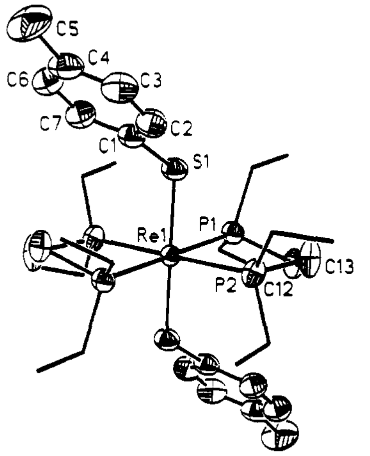

Figure 3. ORTEP diagram of $[Re(SC_6H_5\text{-}p\text{-}CH_3)_2(DEPE)_2]^+$ with ellipsoids at 50% probability. The Re atom occupies an inversion center. The ethyl substituents on the P atoms have been omitted for clarity but are labeled C8–C11 and C12–C15 in the tables.

somewhat account for the density appearing in this region with reference to a ΔF map.

$\mathbf{[Re^{III}(SC_6H_5)_2(DPPE)_2]CF_3SO_3\cdot{}^1/_2NCCH_3}$. Fractional atomic coordinates are available in Table IX. Selected bond lengths and angles in the cation are contained in Table X. Figure 4 shows the trans-octahedral geometry and atom labeling about Re1. The coordination about Re2 is similar. In the structure, there are two independent half-cations, each Re atom occupying a crystallographic inversion center. The $CF_3SO_3^-$ anion is severely disordered; no distinction can be made between the CF_3 and the SO_3 ends of the molecule. With this kind of positional disorder, only an averaged amount of electron density is seen in the map, so the S and C atom sites were each assigned to contain $^1/_2$ C and $^1/_2$ S. Likewise the O and F atoms were each indentified as $^1/_2$ O and $^1/_2$ F in the refinement. Lowering the space group does not improve the anion disorder, since an original solution in the acentric space group $P1$ led to identical problems in this region. One-half equivalent of acetonitrile was also found in the lattice.

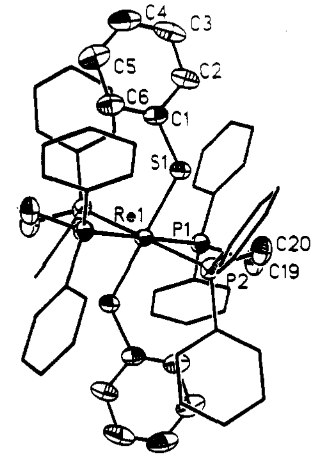

Figure 4. ORTEP diagram of $[Re(SC_6H_5)_2(DPPE)_2]^+$ with ellipsoids at 50% probability. The Re atom occupies an inversion center. The phenyl substitutents on the P atoms have been omitted for clarity but are labeled C7–C12, C13–C18, C21–C26, and C27–C32 in the tables.

Discussion

Synthesis. The title complexes appear to be generated by a reduction–substitution route in which excess thiol both reduces and ligates to a Re(V) starting material ($[ReO_2Py_4]^+$ or $ReOCl_3(PPh_3)_2$); the resulting intermediate then reacts with the bidentate diphosphine ligand DEPE or DPPE. In the ethanethiolate case, the intermediate complex is possibly $[Re^{III}_2(SEt)_4Py_3(O)]$ a species which is observed in the reaction mixture by a positive ion mode FAB-MS. The efficiency of the preparative reaction (in terms of both net yield and reaction rate) decreases in the order of the R group: $C_6H_4\text{-}p\text{-}CH_3 > C_6H_5 > CH_2C_6H_4\text{-}p\text{-}OCH_3 > C_6H_4\text{-}p\text{-}Cl \sim CH_2C_6H_5 \gg C_2H_5$. This order implies that the nucleophilicity of the thiol is an important factor in determining the overall efficiency of the reduction–substitution synthetic reaction.

The efficiency is also sometimes limited by the Re complex used as starting material. Use of $[Re(O)Cl_3(PPh_3)_2]$ leads to formation of $[Re(SR)Cl(DPPE)_2]^+$ in significant amounts when R = $C_6H_4\text{-}p\text{-}CH_3$, C_6H_5, and $C_6H_4\text{-}p\text{-}Cl$. The desired bis(thiolato) product can be obtained in good yield if $[ReO_2Py_4]Cl\cdot 2H_2O$ is used instead. The net isolated yields of the DPPE complexes are generally higher than those of the corresponding DEPE complexes, possibly due to the higher solubility of the latter.

Visible–UV Spectra. The absorption spectra of the thiolato *trans*-$[Re(SR)_2(DIP)_2]^+$ complexes are similar to those of the corresponding *trans*-$[Tc(SR)_2(DIP)_2]^+$ complexes in that both are characterized by intense bands in the visible region.[8,9] In the technetium case, this sulfur-to-Tc charge transfer (CT) band is split into two components, which have been assigned as a S(π)-to-Tc transition at lower energy (ca. 16 000 cm^{-1}) and a less intense S(σ)-to-Tc at higher energy (ca. 28 000 cm^{-1}).[8,9] By analogy, the characteristic intense band of the *trans*-$[Re(SR)_2(DPPE)_2]^+$ complexes is assigned as a S(π)-to-Re CT transition. The corresponding S(σ)-to-Re transition is presumed to be unobserved because of its lower intensity and overlap with transitions in the UV region.

The intense CT band of the red *trans*-$[Re(SR)_2(DIP)_2]^+$ complexes (R = alkyl) occurs at ca. 19 300–19 800 cm^{-1}, significantly higher in energy than observed for the corresponding Tc complexes (ca. 16 400–16 800 cm^{-1}). This observation is consistent with what is seen for the halo complexes, *trans*-$[MX_2(DIP)_2]^+$ (M = Tc, Re; X = Cl, Br; DIP = DEPE, DPPE), where halogen-to-metal CT bands also occur at higher energies for the Re(III) complexes than for the corresponding Tc(III) ones,[6,8] and is understood on the basis that Tc(III) is a stronger oxidant than Re(III) (vide infra). The CT band is somewhat lower in energy for the DEPE complexes than for DPPE complexes; this pattern is again mirrored by the halo complexes. For both the

Table IX. Fractional Atomic Coordinates for [Re(SC$_6$H$_5$)$_2$(DPPE)$_2$](CR$_3$SO$_3$)·$^1/_2$NCCH$_3$

atom	*x*	*y*	*z*	atom	*x*	*y*	*z*
Re1	0.00000	0.00000	0.00000	C37	0.8948 (4)	−0.8586 (4)	0.4412 (3)
S1	−0.0398 (2)	0.1468 (2)	0.0605 (1)	C38	0.7932 (4)	−0.7724 (4)	0.4640 (3)
C1	−0.1729 (4)	0.2504 (4)	0.0919 (3)	P3	0.4214 (2)	−0.4780 (2)	0.6283 (1)
C2	−0.1662 (4)	0.3489 (4)	0.0994 (3)	C39	0.4539 (5)	−0.5936 (5)	0.6992 (3)
C3	−0.2645 (4)	0.4368 (4)	0.1243 (3)	C40	0.5592 (5)	−0.6369 (5)	0.7157 (3)
C4	−0.3697 (4)	0.4262 (4)	0.1418 (3)	C41	0.5807 (5)	−0.7220 (5)	0.7703 (3)
C5	−0.3764 (4)	0.3276 (4)	0.1343 (3)	C42	0.4969 (5)	−0.7638 (5)	0.8086 (3)
C6	−0.2781 (4)	0.2397 (4)	0.1093 (3)	C43	0.3916 (5)	−0.7206 (5)	0.7921 (3)
P1	0.1490 (2)	0.0642 (2)	−0.0825 (1)	C44	0.3701 (5)	−0.6355 (5)	0.7375 (3)
C7	0.1144 (6)	0.2132 (4)	−0.1025 (3)	C45	0.2690 (4)	−0.4104 (5)	0.6617 (3)
C8	0.1195 (6)	0.2737 (4)	−0.0550 (3)	C46	0.2238 (4)	−0.3310 (5)	0.7095 (3)
C9	0.0891 (6)	0.3877 (4)	−0.0695 (3)	C47	0.1070 (4)	−0.2864 (5)	0.7373 (3)
C10	0.0537 (6)	0.4412 (4)	−0.1315 (3)	C48	0.0354 (4)	−0.3211 (5)	0.7172 (3)
C11	0.0487 (6)	0.3808 (4)	−0.1790 (3)	C49	0.0806 (4)	−0.4006 (5)	0.6694 (3)
C12	0.0790 (6)	0.2668 (4)	−0.1646 (3)	C50	0.1974 (4)	−0.4452 (5)	0.6417 (3)
C13	0.2187 (5)	0.0226 (5)	−0.1729 (3)	C51	0.4867 (9)	−0.3928 (9)	0.6484 (5)
C14	0.3239 (5)	0.0313 (5)	−0.2055 (3)	C52	0.4783 (9)	−0.2930 (9)	0.5954 (5)
C15	0.3760 (5)	0.0078 (5)	−0.2758 (3)	P4	0.5198 (2)	−0.3237 (2)	0.5015 (1)
C16	0.3228 (5)	−0.0244 (5)	−0.3136 (3)	C53	0.6626 (4)	−0.3183 (6)	0.4683 (4)
C17	0.2176 (5)	−0.0330 (5)	−0.2810 (3)	C54	0.6947 (4)	−0.2738 (6)	0.3984 (4)
C18	0.1655 (5)	−0.0095 (5)	−0.2106 (3)	C55	0.8055 (4)	−0.2773 (6)	0.3704 (4)
C19	0.2723 (9)	0.0167 (9)	−0.0432 (5)	C56	0.8841 (4)	−0.3252 (6)	0.4122 (4)
C20	0.2401 (9)	−0.0011 (9)	0.0353 (5)	C57	0.8520 (4)	−0.3697 (6)	0.4820 (4)
P2	0.1487 (2)	−0.0838 (2)	0.0666 (1)	C58	0.7412 (4)	−0.3662 (6)	0.5100 (4)
C21	0.2444 (5)	−0.2243 (4)	0.0579 (4)	C59	0.4401 (5)	−0.1899 (4)	0.4589 (3)
C22	0.3594 (5)	−0.2567 (4)	0.0541 (4)	C60	0.4236 (5)	−0.0935 (4)	0.4847 (3)
C23	0.4279 (5)	−0.3682 (4)	0.0563 (4)	C61	0.3657 (5)	0.0089 (4)	0.4523 (3)
C24	0.3814 (5)	−0.4473 (4)	0.0622 (4)	C62	0.3243 (5)	0.0148 (4)	0.3941 (3)
C25	0.2663 (5)	−0.4150 (4)	0.0660 (4)	C63	0.3407 (5)	−0.0816 (4)	0.3684 (3)
C26	0.1978 (5)	−0.3034 (4)	0.0638 (4)	C64	0.3987 (5)	−0.1840 (4)	0.4008 (3)
C27	0.1229 (6)	−0.0838 (5)	0.1640 (2)	C/S3	0.371 (2)	0.138 (2)	0.164 (1)
C28	0.1157 (6)	0.0069 (5)	0.1921 (2)	F/O1	0.273 (2)	0.173 (2)	0.220 (1)
C29	0.1000 (6)	0.0042 (5)	0.2653 (2)	F/O2	0.473 (3)	0.188 (3)	0.126 (2)
C30	0.0913 (6)	−0.0893 (5)	0.3104 (2)	F/O3	0.381 (2)	0.048 (2)	0.134 (1)
C31	0.0985 (6)	−0.1800 (5)	0.2822 (2)	C/S4	0.279 (1)	0.250 (1)	0.1067 (8)
C32	0.1143 (6)	−0.1773 (5)	0.2090 (2)	F/O4	0.177 (1)	0.234 (1)	0.1140 (7)
Re2	0.50000	−0.50000	0.50000	F/O5	0.252 (3)	0.343 (3)	0.135 (2)
S2	0.6675 (2)	−0.5799 (2)	0.5355 (1)	F/O6	0.379 (2)	0.202 (2)	0.039 (1)
C33	0.7893 (4)	−0.6965 (4)	0.5044 (3)	N1	0.835 (2)	0.488 (2)	0.663 (1)
C34	0.8871 (4)	−0.7068 (4)	0.5221 (3)	C65	0.785 (2)	0.520 (2)	0.706 (1)
C35	0.9887 (4)	−0.7929 (4)	0.4994 (3)	C66	0.714 (4)	0.570 (4)	0.753 (2)
C36	0.9926 (4)	−0.8688 (4)	0.4589 (3)				

Table X. Selected Bond Lengths (Å) and Angles (deg) in [Re^{III}(SC$_6$H$_5$)$_2$(DPPE)$_2$]$^+$

Re1–S1	2.305 (4)	Re2–S3	2.301 (3)
Re1–P1	2.486 (3)	Re2–P3	2.465 (4)
Re1–P2	2.459 (3)	Re2–P4	2.478 (4)
S1–C1	1.774 (7)	S3–C33	1.785 (7)
Re1–S1–C1	128.5 (3)	Re2–S3–C33	128.8 (3)
Re1–P1–C7	120.1 (3)	Re2–P3–C39	123.3 (3)
Re1–P1–C13	123.3 (3)	Re2–P3–C45	119.5 (4)
Re1–P1–C19	109.5 (5)	Re2–P3–C51	105.6 (5)
Re1–P2–C20	106.1 (5)	Re2–P3–C52	108.4 (5)
Re1–P2–C21	120.2 (4)	Re2–P3–C53	117.6 (3)
Re1–P2–C27	124.3 (2)	Re2–P3–C59	124.5 (3)
S1–Re1–P1	84.1 (1)	S3–Re2–P3	81.9 (1)
S1–Re1–P2	80.7 (1)	S3–Re2–P4	84.6 (1)
P1–Re1–P2	80.1 (1)	P3–Re2–P4	80.9 (1)

DEPE and DPPE complexes the CT band energy decreases in the order SC$_2$H$_5$ > SCH$_2$C$_6$H$_5$ > SCH$_2$C$_6$H$_4$-*p*-OCH$_3$.

The blue *trans*-[Re(SR)$_2$(DPPE)$_2$]$^+$ (R = aryl) complexes exhibit the intense CT band at ca. 16 100–16 500 cm^{-1}, while the purple *trans*-[Re(SR)$_2$(DEPE)$_2$]$^+$ (R = aryl) complexes exhibit an intense band at ca. 17 400 cm^{-1} and a shoulder at ca. 19 200–19 400 cm^{-1}; this shoulder is not observed in the case of the red *trans*-[Re(SR)$_2$(DEPE)$_2$]$^+$ (R = alkyl) complexes. It is interesting to note that analogous *cis*-[Tc(SR)$_2$(DIP)$_2$]$^+$ complexes also exhibit a shoulder in this region.[10,11] For both the DEPE and DPPE Re(III) complexes, the CT band energy decreases in the order SC$_6$H$_5$ > SC$_6$H$_4$-*p*-Cl > SC$_6$H$_4$-*p*-CH$_3$.

The *trans*-[Re(SR)$_2$(DIP)$_2$]$^+$ complexes also exhibit intense bands in the UV region, but the spectral behavior in this region is sensitive to the nature of the thiolato ligands. In the analogous *trans*-[Tc(SR)$_2$(DIP)$_2$]$^+$ (DIP = DMPE and DEPE) complexes, the UV region is populated by phosphorus-to-Tc charge-transfer bands.[8-11] Thus, it is likely that the complex pattern of bands observed in the UV region for *trans*-[Re(SR)$_2$(DIP)$_2$]$^+$ arises from phosphorus-to-Re charge-transfer transitions superimposed on transitions specific to the particular coordinated thiolato ligand.

Electrochemistry. The data of Table IV show that the Re(III/II) potential values for *trans*-[Re(SR)$_2$(DPPE)$_2$]$^{+}$1/^{0} complexes are much more negative (ca. 240–540 mV) than that for the corresponding chloro complex, *trans*-[ReCl$_2$(DPPE)$_2$]$^{+/0}$ ($E^{\circ\prime}$(Re(III/II)) = −0.297 V).[6] The same trend is observed for the Re(II/I) couples,[6] and the potential differences are about the same. Thus, for both the Re(III/II) and Re(II/I) couples, replacement of chloride ligands by strongly σ-donating thiolate ligands within the *trans*-[Re(X)$_2$(DIP)$_2$]$^{+/0/-}$ core dramatically stabilizes the higher oxidation state. This effect makes it possible to observe the Re(IV/III) couple for some of the thiolato complexes.

Ease of reduction of the Re center increases in the order SC$_2$H$_5$ < SCH$_2$C$_6$H$_4$-*p*-OCH$_3$ < SCH$_2$C$_6$H$_5$ < SC$_6$H$_4$-*p*-CH$_3$ < SC$_6$H$_5$ < SC$_6$H$_4$-*p*-Cl, the same as that observed in the corresponding *trans*-[Tc(SR)$_2$(DMPE)$_2$]$^{+/0}$ complexes.[8] Due to their enhanced π-acidity, arenethiolato complexes exhibit more positive Re(III/II) potentials than do alkane- or phenylmethanethiolato complexes. Individual arenethiolato complexes illustrate the same behavior on a smaller scale; ease of reduction of Re(III) increases in the order *p*-CH$_3$ < *p*-H < *p*-Cl.

In the case of the halide complexes, [M(X)$_2$(DIP)$_2$]$^{+/0}$ (M = Re, Tc; X = Cl, Br; DIP = DPPE, DEPE), the M(III/II) the greater π-acidity of DPPE $E^{\circ\prime}$ causes values of the DPPE com-

Table XI. Structural Parameters for *trans*-$[ReX_2(DIP)_2]^{n+}$ Complexes[a]

	Re–X, Å	Re–P, Å	P–Re–P bite angle, deg	ref
$[Re^{III}Cl_2(DMPE)_2]^+$	2.337 (1)	2.438 (2)	81.4 (2)	4
$[Re^{III}Cl_2(DEPE)_2]^+$	2.335 (3)	2.450 (6)	81.5 (1)	20
$[Re^{III}Cl_2(DTPE)_2]^+$	2.310 (1)	2.489 (7)	81.0 (1)	20
$[Re^{II}Cl_2(DPPEE)_2]^0$	2.422 (2)	2.405 (2)	78.8 (1)	21
$[Re^{III}(SC_6H_5)_2(DEPE)_2]^+$	2.305 (1)	2.453 (18)	81.47 (4)	*b*
$[Re^{III}(SC_6H_4\text{-}p\text{-}CH_3)_2(DEPE)_2]^+$	2.321 (1)	2.452 (30)	80.78 (4)	*b*
$[Re^{III}(SC_6H_5)_2(DPPE)_2]^+$	2.303 (3)	2.472 (12)	80.5 (5)	*b*

[a] DMPE = 1,2-bis(dimethylphosphino)ethane; DEPE = 1,2-bis(diethylphosphino)ethane; DTPE = 1,2-bis(di-*p*-tolylphosphino)ethane; DPPEE = 1,2-bis(diphenylphosphino)ethene; DPPE = 1,2-bis(diphenylphosphino)ethane. [b] This work.

plexes to be 230–260 mV more positive than those of the DEPE complexes.[8,12] This same trend is observed within the *trans*-$[Re(SR)_2(DIP)_2]^{+/0}$ complexes studied herein. For the alkane- and phenylmethanethiolato complexes, the differences in Re(III/II) values between the DPPE and DEPE complexes are in the range 150–170 mV. However, for the arenethiolato complexes this difference is only 15 – 90 mV, presumably because the arenethiolato ligand itself provides sufficient π-acid character to level the different π-acidities of DPPE and DEPE.[8-11]

In general, M(III) (M = Tc, Re) DEPE complexes are more difficult to reduce than the DMPE analogues[8-12] because DEPE is a better σ-donor ligand. For the M(III/II) couple, this effect averages about 31 mV for *trans*-$[TcX_2(DIP)_2]^{+/0}$ (X = Cl, Br) complexes and about 27 mV for the analogous Re complexes.[8-12] However, this relatively small effect is even further diminished when X is a strongly σ-donating thiolato ligand, possibly due to saturation of the σ-accepting ability of the metal center.[8,9] Thus, it is possible to estimate the average $E^{\circ\prime}$ difference which results from varying M in trans-$[MX_2(DIP)_2]^{+/0}$ (M = Tc, Re) complexes by comparison of relevant Tc/Re pairing wherein X is constant and DIP is either DMPE or DEPE. For eight couples wherein X = Cl, Br, $SC_6H_4\text{-}p\text{-}CH_3$, $SC_6H_4\text{-}p\text{-}Cl$, SC_6H_5, $SCH_2C_6H_4\text{-}p\text{-}OCH_3$, $SCH_2C_6H_5$, or SC_2H_5, the average potential difference $E^{\circ\prime}(Tc) - E^{\circ\prime}(Re)$ is 271 ± 55 mV. For the halo complexes *trans*-$[M(X)_2(DIP)_2]^{+/0/-}$ wherein X is either Cl or Br and DIP is varied (DIP = DEPE, DMPE, DPPE, DIARS), the average potential difference for M(III/II) and M(II/I) couples between Re and Tc complexes has been reported[6] as 219 ± 15 mV. Thus, for *trans*-$[M(X)_2(DIP)_2]^{+/0}$ complexes in general, the Re(III) complex is consistently about 220-270 mV more difficult to reduce than the Tc(III) analogue.

Crystallography. There have been only a few $[ReX_2(DIP)_2]^{n+}$ complexes structurally characterized before this study, and all contain X = Cl[4,20,21] (see Table XI). This is in contrast to the more extensively characterized $[TcX_2(DIP)_2]^{n+}$ complexes, the radiopharmaceutical potential of which sparked considerable interest a few years ago.[6,7] Table XI compares bond parameters for the previously characterized $[ReCl_2(DIP)_2]^{n+}$ complexes and those for the $[Re(SR)_2(DIP)_2]^+$ complexes characterized herein. The Re–P distances are sensitive to oxidation state; the Re(II)–P distance is shorter than the Re(III)–P distance as expected for bonds wherein covalent M → L back-bonding is paramount (correspondingly, the Re(II)–Cl distance is longer than the Re(III)–Cl distance as expected for bonds wherein electrostatic interactions are predominant). The Re^{III}–P lengths increase with increasing bulk of the phosphine R substituent ($R_2PCH_2CH_2PR_2$): 2.44 Å for DMPE (R = Me), 2.45 Å for DEPE (R = Et), 2.47 Å for DPPE (R = Ph), and 2.49 Å for DTPE (R = *p*-toluene). This trend parallels that found for analogous Tc complexes.[8] The higher standard deviations associated with the Re–P lengths reported in this work (compared with the other entries of Table XI) result from averaging nonequivalent Re–P lengths which in turn result from a skew distortion also noted in thiolato–Tc–DIP complexes.[8] The chelate P–Re–P bite angles are all similar (average 81.1 (4)°) with the exception of that for the $[Re^{II}Cl_2(DPPEE)_2]$ complex, which contains a double bond in the C–C backbone that necessarily reduces the bite angle.

The Re-S bond lengths are relatively insensitive to the identity of the DIP ligands; Re–SPh = 2.305 (1) and 2.303 (3) Å for $[Re(SPh)_2(DIP)_2]^+$ with DIP = DEPE and DPPE, respectively. However, the Re–S distances are dependent on the nature of the organic moiety bonded to the sulfur atom; for the two *trans*-$[Re(SR')_2(DEPE)_2]^+$ complexes, Re–S is 2.305 (1) Å when R' = C_6H_5 and 2.321 (1) Å when R' is $C_6H_4\text{-}p\text{-}CH_3$. The associated S–C bonds are also dependent on the nature of the organic moiety; S–C is 1.786 (5) Å when R' = C_6H_5 and 1.800 (5) Å when R' is $C_6H_4\text{-}p\text{-}CH_3$. Apparently, the more electron-donating *p*-CH_3 group changes the energies of the bonding orbital set in a manner which causes a general weakening of the Re–S–C bond system.

Analogous $[M(SR)_2(DIP)_2]^+$ (M = Tc, Re) complexes exhibit remarkably similar bond lengths. For example, *trans*-$[Tc(SCH_3)_2(DEPE)_2]^+$[8] has Tc–P = 2.45 (1) Å, which is identical to the Re–P(DEPE) distances of Table XI. The Re–SPh bond lengths (2.303 Å and 2.305 Å) are in close agreement with Tc–SR distances in *trans*-$[Tc(SCH_3)_2(DMPE)_2]^+$ (2.300 (3) Å)[8], *trans*-$[Tc(SCH_3)_2(DEPE)_2]^+$ (2.303 (1) Å)[8], and *cis*-$[Tc(SPh)_2(DEPE)_2]^+$ (2.289 (7) Å)[11].

A major point of interest resulting from structural studies of $[M(SPh)_2(DEPE)_2]^+$ (M = Tc, Re) complexes is that the two isolated Re species adopt the trans configuration whereas the Tc analog exhibits the cis configuration[8] (in the Re system only the trans complex is observed, while in the Tc system both cis and trans complexes are observed). Following the arguments presented by Pramanik[22] on Os(II) and Os(III) complexes which contain both P-donating and S-donating ligands, this observation implies that π-back-bonding is more prevalent in the Tc(III) system than in the analogous Re(III) system. For Tc(III) there appears to be a balance between the demands of π-back-bonding (which favor the cis configuration by placing two sulfur atoms trans to the π-acid P atoms) and steric hindrance (which favors the trans configuration), while for Re(III) the steric requirements appear to dominate and only the trans configuration is observed. Since bond lengths and angles in the Tc and Re systems are nearly identical, steric requirements within the two systems must be very similar. Thus, π-back-bonding in the Re(III) system appears to be less important than in the analogous Tc(III) system. Interestingly, this same conclusion has been reached independently through an electrochemical parametrization analysis of rhenium and technetium redox couples.[23] Carried one step further, this conclusion about the relative effectiveness of π-back-bonding in Re(III) and Tc(III) phosphine complexes implies that the radial extension of the Re(III) 5d orbitals is too large to permit the efficient overlap with P-based orbitals that is observed for the Tc(III) 4d orbitals.

Acknowledgment. Financial support by the National Institutes of Health (Grant HL-21276) is gratefully acknowledged. The diffractometer used herein was purchased through an NSF equipment grant to Wayne State University.

Supplementary Material Available: Listings of thermal parameters, hydrogen parameters, and bond lengths and angles for *trans*-$[Re(SC_6H_5)_2(Et_2PCH_2CH_2PEt_2)_2]PF_6$ (Tables A–C), *trans*-$[Re(SC_6H_4\text{-}p\text{-}CH_3)_2(Et_2PCH_2CH_2PEt_2)_2]PF_6$ (Tables E–G), and *trans*-$[Re(SC_6H_5)_2(Ph_2PCH_2CH_2PPh_2)_2]CF_3SO_3\cdot{}^1/_2(NCCH_3)$ (Tables I–K) (14 pages); listings of calculated and observed structure factors for the three complexes (Tables D, H, and L) (76 pages). Ordering information is given on any current masthead page.

---

(20) Cotton, F. A.; Daniels, L. M. *Inorg. Chim. Acta* **1988**, *142*, 255.

(21) Barkir, M.; Fanwick, P. E.; Walton, R. A. *Polyhedron* **1987**, *6*, 907.

(22) Pramanik, A.; Bag, N.; Ray, D.; Lahiri, G. K.; Chakravorty, A. *Inorg. Chem.* **1991**, *30*, 410.

(23) Lever, A. B. P. *Inorg. Chem.* **1991**, *30*, 1980.